

The Beaker Phenomenon and the Genomic Transformation of Northwest Europe

Iñigo Olalde¹, Selina Brace², Morten E. Allentoft³, Ian Armit^{4,*}, Kristian Kristiansen^{5,*}, Nadin Rohland¹, Swapan Mallick^{1,6,7}, Thomas Booth², Anna Szécsényi-Nagy⁸, Alissa Mittnik^{9,10}, Eveline Altena¹¹, Mark Lipson¹, Iosif Lazaridis^{1,6}, Nick Patterson⁶, Nasreen Broomandkhoshbacht^{1,7}, Yoan Diekmann¹², Zuzana Faltyskova¹², Daniel Fernandes^{13,14}, Matthew Ferry^{1,7}, Eadaoin Harney¹, Peter de Knijff¹¹, Megan Michel^{1,7}, Jonas Oppenheimer^{1,7}, Kristin Stewardson^{1,7}, Alistair Barclay¹⁵, Kurt W. Alt^{16,17,18}, Azucena Avilés Fernández¹⁹, Eszter Bánffy^{20,21}, Maria Bernabò-Brea²², David Billoin²³, Concepción Blasco²⁴, Clive Bonsall²⁵, Laura Bonsall²⁶, Tim Allen²⁷, Lindsey Büster⁴, Sophie Carver²⁸, Laura Castells Navarro⁴, Oliver Edward Craig²⁹, Gordon T. Cook³⁰, Barry Cunliffe³¹, Anthony Denaire³², Kirsten Egging Dinwiddy¹⁵, Natasha Dodwell³³, Michal Ernée³⁴, Christopher Evans³⁵, Milan Kuchařík³⁶, Joan Francès Farré³⁷, Harry Fokkens³⁸, Chris Fowler³⁹, Michiel Gazenbeek⁴⁰, Rafael Garrido Pena²⁴, María Haber-Uriarte¹⁹, Elżbieta Haduch⁴¹, Gill Hey²⁷, Nick Jowett⁴², Timothy Knowles⁴³, Ken Massy⁴⁴, Saskia Pfrengle⁴⁵, Philippe Lefranc⁴⁶, Olivier Lemercier⁴⁷, Arnaud Lefebvre^{48,49}, Joaquín Lomba Maurandi¹⁹, Tona Majó⁵⁰, Jacqueline I. McKinley¹⁵, Kathleen McSweeney²⁵, Mende Balázs Gusztáv⁸, Alessandra Modi⁵¹, Gabriella Kulcsár²⁰, Viktória Kiss²⁰, András Czene⁵², Róbert Patay⁵³, Anna Endrődi⁵⁴, Kitti Köhler²⁰, Tamás Hajdu^{55,56}, João Luís Cardoso^{57,58}, Corina Liesau²⁴, Michael Parker Pearson⁵⁹, Piotr Włodarczak⁶⁰, T. Douglas Price⁶¹, Pilar Prieto⁶², Pierre-Jérôme Rey⁶³, Patricia Ríos²⁴, Roberto Risch⁶⁴, Manuel A. Rojo Guerra⁶⁵, Aurore Schmitt⁶⁶, Joël Serrallongue⁶⁷, Ana Maria Silva¹⁴, Václav Smrčka⁶⁸, Luc Vergnaud⁶⁹, João Zilhão^{57,70,71}, David Caramelli⁵¹, Thomas Higham⁷², Volker Heyd^{28,73}, Alison Sheridan⁷⁴, Karl-Göran Sjögren⁵, Mark G. Thomas¹², Philipp W. Stockhammer^{44,75}, Ron Pinhasi^{13,76}, Johannes Krause⁷⁵, Wolfgang Haak^{75,77,*}, Ian Barnes^{2,*}, Carles Lalueza-Fox^{78,*}, David Reich^{1,6,7,*}

*Principal investigators who contributed centrally to this study

To whom correspondence should be addressed: D.R. (reich@genetics.med.harvard.edu), I.O. (inigo_olalde@hms.harvard.edu)

¹Department of Genetics, Harvard Medical School, Boston, Massachusetts 02115, USA, ²Department of Earth Sciences, Natural History Museum, London SW7 5BD, UK, ³Centre for GeoGenetics, Natural History Museum, University of Copenhagen, Copenhagen 1350, Denmark, ⁴School of Archaeological Sciences, University of Bradford, Bradford BD7 1DP, UK, ⁵University of Gothenburg, Gothenburg 405 30, Sweden, ⁶Broad Institute of MIT and Harvard, Cambridge, Massachusetts 02142, USA, ⁷Howard Hughes Medical Institute, Harvard Medical School, Boston, Massachusetts 02115, USA, ⁸Laboratory of Archaeogenetics, Institute of Archaeology, Research Centre for the Humanities, Hungarian Academy of Sciences, Budapest

1097, Hungary, ⁹Institute for Archaeological Sciences, Archaeo- and Palaeogenetics, University of Tübingen, Tübingen 72070, Germany, ¹⁰Department of Archaeogenetics, Max Planck Institute for the Science of Human History, 07745 Jena, Germany, ¹¹Department of Human Genetics, Leiden University Medical Center, Leiden 2333, The Netherlands, ¹²Research Department of Genetics, Evolution and Environment, University College London, London WC1E 6BT, UK, ¹³School of Archaeology and Earth Institute, University College Dublin, Dublin 4, Ireland, ¹⁴Research Center for Anthropology and Health, Department of Life Science, University of Coimbra, Coimbra 3000-456, Portugal, ¹⁵Wessex Archaeology, Salisbury SP4 6EB, UK, ¹⁶Center of Natural and Cultural History of Man, Danube Private University, Krems 3500, Austria, ¹⁷Department of Biomedical Engineering, Basel University, Basel 4123, Switzerland, ¹⁸Integrative Prehistory and Archaeological Science, Basel University, Switzerland, ¹⁹Área de Prehistoria, Universidad de Murcia, Murcia 30001, Spain, ²⁰Institute of Archaeology, Research Centre for the Humanities, Hungarian Academy of Sciences, Budapest 1097, Hungary, ²¹Romano-Germanic Commission, German Archaeological Institute, Frankfurt/Main 60325, Germany, ²²Museo Archeologico Nazionale di Parma, Parma 43100, Italy, ²³INRAP, Institut National de Recherches Archéologiques Préventives, Buffard 25440, France, ²⁴Departamento de Prehistoria y Arqueología, Universidad Autónoma de Madrid, Madrid 28049, Spain, ²⁵School of History, Classics and Archaeology, University of Edinburgh, Edinburgh EH8 9AG, UK, ²⁶Independent Researcher, 10 Merchiston Gardens, Edinburgh EH10 5DD, UK, ²⁷Oxford Archaeology, Oxford, OX2 0ES, UK, ²⁸Department of Archaeology and Anthropology, University of Bristol, Bristol BS8 1UU, UK, ²⁹BioArCh, Department of Archaeology, University of York, York, YO10 5DD, UK, ³⁰Scottish Universities Environmental Research Centre East Kilbride G75 0QF, UK, ³¹Institute of Archaeology, University of Oxford, Oxford OX1 2PG, UK, ³²Université de Strasbourg, Strasbourg 67081, France, ³³Oxford Archaeology East, Cambridge CB23 8SQ, UK, ³⁴Institute of Archaeology, Czech Academy of Sciences, Prague 118 01, Czech Republic, ³⁵Cambridge Archaeological Unit, Department of Archaeology, University of Cambridge, Cambridge CB3 0DT, UK, ³⁶Labrys o.p.s. Prague 198 00, Czech Republic, ³⁷Museu i Poblats Ibèrics de Ca n'Oliver, Cerdanyola del Vallès 08290, Spain, ³⁸Faculty of Archaeology, Leiden University, 2333 CC Leiden, The Netherlands, ³⁹School of History, Classics & Archaeology, Newcastle University, Newcastle Upon Tyne NE1 7RU, UK, ⁴⁰INRAP, Institut National de Recherches Archéologiques Préventives, Nice 06300, France, ⁴¹Institute of Zoology and Biomedical Research, Jagiellonian University, Cracow 31-007, Poland, ⁴²Great Orme Mines, Great Orme, Llandudno LL30 2XG, UK, ⁴³Bristol Radiocarbon Accelerator Mass Spectrometry Facility, University of Bristol, Bristol BS8 1UU, UK, ⁴⁴Institut für Vor- und Frühgeschichtliche Archäologie und Provinzialrömische Archäologie, Ludwig-Maximilians-Universität München, Munich 80539, Germany, ⁴⁵Institute for Archaeological Sciences, Eberhard-Karls-University of Tübingen, Tübingen 72070, Germany, ⁴⁶INRAP, Institut National de Recherches Archéologiques Préventives, Strasbourg 67100, France, ⁴⁷Université Paul-Valéry - Montpellier 3, UMR 5140 ASM, Montpellier 34199, France, ⁴⁸INRAP, Institut National de Recherches Archéologiques Préventives, Metz 57063, France, ⁴⁹UMR 5199, Pacea, équipe A3P, Université de Bordeaux, Talence 33400, France, ⁵⁰Archeom. Departament de Prehistòria, Universitat Autònoma de Barcelona, Cerdanyola del Vallès 08193, Spain, ⁵¹Department of Biology, University of Florence, Florence 50121, Italy, ⁵²Salisbury Ltd., Budaörs 2040, Hungary, ⁵³Ferenczy Museum Center, Szentendre 2100, Hungary, ⁵⁴Budapest History Museum, Budapest 1014, Hungary, ⁵⁵Department of Biological Anthropology, Eötvös Loránd University, Budapest 1117, Hungary, ⁵⁶Hungarian Natural History Museum, Budapest 1083, Hungary, ⁵⁷Centro de Arqueologia, Universidade de Lisboa, Lisboa 1600-214, Portugal, ⁵⁸Universidade Aberta, Lisboa 1269-001, Portugal, ⁵⁹Institute of Archaeology, University College London, London WC1H 0PY, UK, ⁶⁰Institute of Archaeology and Ethnology, Polish Academy of Sciences, Kraków 31-016, Poland, ⁶¹Laboratory for Archaeological Chemistry, University of Wisconsin-Madison, Madison, Wisconsin 53706, USA, ⁶²University of Santiago de Compostela, Santiago de Compostela 15782, Spain, ⁶³UMR 5204 Laboratoire Edytem, Université Savoie Mont Blanc, Chambéry 73376, France, ⁶⁴Departament de Prehistòria, Universitat Autònoma de Barcelona, Cerdanyola del Vallès 08193, Spain, ⁶⁵Department of Prehistory and Archaeology, Faculty of Philosophy and Letters, Valladolid University, Valladolid 47011, Spain, ⁶⁶UMR 7268 ADES, CNRS, Aix-Marseille Univ, EFS, Faculté de médecine Nord, Marseille 13015, France, ⁶⁷Service archéologique, Conseil Général de la Haute-Savoie, Chambéry 73000, France, ⁶⁸Institute for History of Medicine and Foreign Languages, First Faculty of Medicine, Charles University, Prague 121 08, Czech Republic, ⁶⁹ANTEA Bureau d'étude en Archéologie, Habsheim 68440, France, ⁷⁰Institució Catalana de Recerca i Estudis Avançats, Barcelona 08010, Spain, ⁷¹Departament d'Història i Arqueologia, Universitat de Barcelona, Barcelona 08001, Spain, ⁷²Oxford Radiocarbon Accelerator Unit, RLHA, University of Oxford, Oxford OX1 3QY, UK, ⁷³Department of Philosophy, History, Culture and Art Studies, Section of Archaeology, University of Helsinki, Helsinki 00014, Finland, ⁷⁴National Museums Scotland, Edinburgh EH1 1JF, UK, ⁷⁵Max Planck Institute for the Science of Human History, Jena 07745, Germany, ⁷⁶Department of Anthropology, University of Vienna, Vienna 1090, Austria, ⁷⁷Australian Centre for Ancient DNA, School of Biological Sciences, University of Adelaide, Adelaide 5005, Australia, ⁷⁸Institute of Evolutionary Biology, CSIC-Universitat Pompeu Fabra, Barcelona 08003, Spain.

Bell Beaker pottery spread across western and central Europe beginning around 2750 BCE before disappearing between 2200–1800 BCE. The mechanism of its expansion is a topic of long-standing debate, with support for both cultural diffusion and human migration. We present new genome-wide ancient DNA data from 170 Neolithic, Copper Age and Bronze Age Europeans, including 100 Beaker-associated individuals. In contrast to the Corded Ware Complex, which has previously been identified as arriving in central Europe following migration from the east, we observe limited genetic affinity between Iberian and central European Beaker Complex-associated individuals, and thus exclude migration as a significant mechanism of spread between these two regions. However, human migration did have an important role in the further dissemination of the Beaker Complex, which we document most clearly in Britain using data from 80 newly reported individuals dating to 3900–1200 BCE. British Neolithic farmers were genetically similar to contemporary populations in continental Europe and in particular to Neolithic Iberians, suggesting that a portion of the farmer ancestry in Britain came from the Mediterranean rather than the Danubian route of farming expansion. Beginning with the Beaker period, and continuing through the Bronze Age, all British individuals harboured high proportions of Steppe ancestry and were genetically closely related to Beaker-associated individuals from the Lower Rhine area. We use these observations to show that the spread of the Beaker Complex to Britain was mediated by migration from the continent that replaced >90% of Britain’s Neolithic gene pool within a few hundred years, continuing the process that brought Steppe ancestry into central and northern Europe 400 years earlier.

During the third millennium Before the Common Era (BCE), two new archaeological pottery styles expanded across Europe, replacing many of the more localized styles that preceded them¹. The “Corded Ware Complex” in central, northern and eastern Europe was associated with people who derived most of their ancestry from eastern European Yamnaya steppe pastoralists^{2–4}. Bell Beaker pottery is known from around 2750 cal BCE^{5,6} in Atlantic Iberia, although its exact origin is still a matter of debate^{7,8}. By 2500 BCE, it is possible to distinguish in many regions the “Beaker Complex”, defined by assemblages of grave goods including stylised bell-shaped pots, distinctive copper daggers, arrowheads, stone wristguards and V-perforated buttons⁹. Regardless of the geographic region where it originated (if it did have a single origin), elements of the Beaker Complex rapidly spread throughout western Europe (and northern Africa), reaching southern and Atlantic France, Italy and central Europe^{10–12} where they overlapped geographically with the Corded Ware Complex, and from there expanding to Britain and Ireland^{13,14}. A major debate has centred on whether the spread of the Beaker Complex was mediated by the movement of people, culture, or a combination of these^{15–18}. Genome-wide data have revealed high proportions of Steppe ancestry in Beaker Complex-associated individuals

from Germany and the Czech Republic²⁻⁴, consistent with their being a mixture of populations from the Steppe and the preceding farmers of Europe. However, a deeper understanding of the ancestry of people associated with the Beaker Complex requires genomic characterization of individuals across the geographic range and temporal duration of this archaeological phenomenon.

Ancient DNA data and authenticity

To understand the genetic structure of ancient people associated with the Beaker Complex and their relationship to preceding, subsequent and contemporary peoples, we enriched ancient DNA libraries for sequences overlapping 1,233,013 single nucleotide polymorphisms (SNPs) by hybridization DNA capture^{4,19}, and generated new sequence data from 170 ancient Europeans dating to ~4700–1200 BCE (Supplementary Table 1; Supplementary Information, section 1). We also generated 62 new direct radiocarbon dates (Extended Data Table 1). We filtered out libraries with low coverage (<10,000 SNPs) or evidence of contamination (Methods) to obtain a final set of 166 individuals: 97 Beaker-associated individuals and 69 from other ancient populations (Fig. 1b; Extended Data Table 2), including 61 individuals from Neolithic and Bronze Age Britain. We combined our data with previously published ancient DNA data^{2-4,20-37} to form a genome-wide dataset of 476 ancient individuals (Supplementary Table 1). The combined dataset included Beaker-associated individuals from Iberia (n=20), southern France (n=4), northern Italy (n=1), central Europe (n=56), The Netherlands (n=9) and Britain (n=19). We further merged these data with 2,572 present-day individuals genotyped on the Affymetrix Human Origins array^{22,31} and 300 high coverage genomes sequenced as part of the Simons Genome Diversity Project³⁸.

Y-chromosome analysis

We determined Y-chromosome haplogroups for the 54 male Beaker-associated individuals (Supplementary Table 3). Individuals from the Iberian Peninsula carried Y haplogroups known to be common across Europe during the earlier Neolithic period^{2,4,20,26,32,39}, such as I2a (n=3) and G2 (n=1) (Supplementary Table 3). In contrast, Beaker-associated individuals outside Iberia (n=44) largely carried R1b lineages (84%), associated with the arrival of Steppe migrants in central Europe during the Late Neolithic/Early Bronze Age^{2,3}. For individuals in whom we could determine the R1b subtype (n=22), we found that all but one had the derived allele for the R1b-S116/P312 polymorphism, which defines the dominant subtype in western Europe today⁴⁰. Finding this early predominance of the R1b-S116/P312 polymorphism in ancient individuals from central and northwestern Europe suggests that people associated with the Beaker Complex may have had an important role in the dissemination of this lineage throughout most of its present-day distribution.

Genomic insights into the spread of the Beaker Complex

Principal component analysis (PCA) revealed striking heterogeneity among individuals assigned to the Beaker Complex (Fig. 1c, Extended Data Fig. 1a). Genetic differentiation in our dataset was mainly driven by variable amounts of Steppe-related ancestry, with Beaker Complex individuals falling along the axis of variation defined by Yamnaya steppe pastoralists and Middle Neolithic/Copper Age European populations. We obtained qualitatively consistent inferences using ADMIXTURE model-based clustering⁴¹ (Extended Data Fig. 1b).

We grouped Beaker Complex individuals based on geographic proximity and genetic similarity (Supplementary Information, section 4), and used *qpAdm*² to model their ancestry as a mixture of western European hunter-gatherers (WHG), northwestern Anatolian farmers, and Yamnaya steppe pastoralists (the first two of which contributed to earlier European farmers; Supplementary Information, section 6). We find that the great majority of Beaker Complex individuals outside of Iberia derive a large portion of their ancestry from Steppe populations (Fig. 2a), whereas in Iberia, such ancestry is absent in all sampled individuals, with the exception of two (I0461 and I0462) from the Arroyal I site in northern Spain. We detect striking differences in ancestry not only at a pan-European scale, but also within regions and even within sites. Unlike other individuals from the Upper Alsace region of France (n=2), an individual from Hégenheim resembles previous Neolithic populations and can be modelled as a mixture of Anatolian Neolithic and western hunter-gatherers without any Steppe-related ancestry. Given that the radiocarbon date of the Hégenheim individual is older (2832–2476 cal BCE (quoting 95.4% confidence intervals for this and other dates) (Supplementary Information, section 1) than other samples from the same region (2566–2133 cal BCE), the pattern could reflect temporal differentiation. At Szigetszentmiklós in Hungary, we find Beaker Complex-associated individuals with very different proportions (from 0% to 74%) of Steppe ancestry but overlapping dates. This genetic heterogeneity is consistent with early stages of mixture between previously established European farmers and migrants with Steppe ancestry. An implication is that, even at a local scale, the Beaker Complex was associated with people of diverse ancestries.

While the Yamnaya-related ancestry in Beaker Complex associated individuals had an origin in the Steppe^{2,3}, the other ancestry component (from European Neolithic farmers) could potentially be derived from several parts of Europe, as genetically closely related populations were widely distributed across the continent during the Neolithic and Copper Age periods^{2,4,22,25,26,28,32}. To obtain insight into the origin of the Neolithic-related ancestry in Beaker Complex-associated individuals, we began by looking for regional patterns of genetic differentiation within Europe during the Neolithic and Copper Age periods. To study genetic affinity to different Early Neolithic (EN) populations, we computed f_4 -statistics of the form $f_4(\text{Outgroup}, \text{Test}; \text{Iberia_EN},$

LBK_EN) for Neolithic and Copper Age test populations predating the emergence of the Beaker Complex. As previously described², there is genetic affinity to Iberian Early Neolithic farmers in Iberian Middle Neolithic/Copper Age populations, but not in central and northern European Neolithic populations (Fig. 2b), which could be explained by differential affinities to hunter-gatherer individuals from different regions⁴² (Extended Data Fig. 2). A new finding that emerges from our analysis is that Neolithic individuals from southern France and Britain also show a greater affinity to Iberian Early Neolithic farmers than to central European Early Neolithic farmers (Fig. 2b), similar to previous results obtained in a Neolithic farmer genome from Ireland²⁸. By modelling Neolithic populations and WHG in an admixture graph framework, we replicate these results and further show that they are not driven by different proportions of hunter-gatherer admixture (Extended Data Fig. 3; Supplementary Information, section 5). Our results suggest that a portion of the ancestry of the Neolithic farmers of Britain was derived from migrants who spread along the Atlantic coast. Megalithic tombs document substantial interaction along the Atlantic façade of Europe, and our results are consistent with such interactions reflecting movements of people. More data from southern Britain (where our sampling is sparse) and nearby regions in continental Europe will be needed to fully understand the complex interactions between Britain and the continent in the Neolithic⁴³.

The distinctive genetic signatures of pre-Beaker Complex populations in Iberia compared to central Europe allow us to test formally for the origin of the Neolithic farmer-related ancestry in Beaker Complex individuals in our dataset (Supplementary Information, section 6). We grouped individuals from Iberia (n=19) and from outside Iberia (n=84) to increase power, and evaluated the fit of different Neolithic/Copper Age groups with *qpAdm* under the model: Yamnaya + Neolithic/Copper Age. For Beaker Complex individuals from Iberia, the best fit was obtained when Middle Neolithic and Copper Age populations from the same region were used as a source for their Neolithic farmer-related ancestry, and we could exclude central and northern European populations ($P < 4.69\text{E-}03$) (Fig. 2c). Conversely, the Neolithic farmer-related ancestry in Beaker Complex individuals outside Iberia was most closely related to central and northern European Neolithic populations with relatively high hunter-gatherer admixture (e.g. *Globular_Amphora_LN*, $P = 0.14$; *TRB_Sweden_MN*, $P = 0.29$), and we could significantly exclude Iberian sources ($P < 3.18\text{E-}08$) (Fig. 2c). These results support largely different origins for Beaker Complex individuals, with no discernible Iberia-related ancestry outside Iberia.

Nearly complete turnover of ancestry in Britain

British Beaker Complex individuals (n=19) show strong similarities to the central European Beaker Complex both in genetic profile (Extended Data Fig. 1) and in material culture: the great majority of individuals from both regions are associated with “All Over Corded” Beaker

pottery. The presence of large amounts of Steppe-related ancestry in the British Beaker Complex (Fig. 2a) contrasts sharply with Neolithic individuals from Britain (n=35), who have no evidence of Steppe genetic affinities and cluster instead with Middle Neolithic and Copper-Age populations from mainland Europe (Extended Data Fig. 1). Thus, the arrival of Steppe ancestry in Britain was mediated by a migration that began with the Beaker Complex. A previous study showed that Steppe ancestry arrived in Ireland by the Bronze Age²⁸, and here we show that – at least in Britain – it arrived by the Copper Age / Beaker period.

Among the different continental Beaker Complex groups analysed in our dataset, individuals from Oostwoud (Province of Noord-Holland, The Netherlands) are the most closely related to the great majority of the Beaker Complex individuals from southern Britain (n=14). They had almost identical Steppe ancestry proportions (Fig. 2a), the highest shared genetic drift (Extended Data Fig. 4b) and were symmetrically related to other ancient populations using f_4 -statistics (Extended Data Fig. 4a), showing that they are consistent with being derived from the same ancestral population without additional mixture into either group. We next investigated the magnitude of population replacement in Britain with $qpAdm^2$ by modelling Beaker Complex and Bronze Age individuals as a mixture of continental Beaker Complex (using the Oostwoud individuals as a surrogate) and the British Neolithic population (Supplementary Information, section 6). Fig. 3a shows the results of this analysis, ordering individuals by date and showing excess Neolithic ancestry compared to continental Beaker Complex as a baseline. For the earliest individuals (between ~2400–2000 BCE), the Neolithic ancestry excess is highly variable, consistent with migrant communities who were just beginning to mix with the previously established Neolithic population of Britain. During the subsequent Bronze Age we observe less variation among individuals and a modest increase in Neolithic-related ancestry (Fig. 3a), which could represent admixture with persisting populations with high levels of Neolithic-related ancestry (or alternatively incoming continental populations with higher proportions of Neolithic-related ancestry). In either case, our results imply a minimum of $93 \pm 2\%$ local population turnover by the Middle Bronze Age (Supplementary Information, section 6). Specifically, for individuals from Britain around 2000 BCE, at least this fraction of their DNA derives from ancestors who at 2500 BCE lived in continental Europe. An independent line of evidence for population turnover comes from Y-chromosome haplogroup composition: while R1b haplogroups were completely absent in the Neolithic samples (n=25), they represent 95% and 75% of the Y-chromosomes in Beaker Complex-Early Bronze Age and Middle Bronze Age males in Britain, respectively (Fig. 3b; Supplementary Table 3).

Our genetic time transect in Britain also allowed us to track the frequencies of alleles with known phenotypic effects. Derived alleles at rs12913832 (SLC45A2) and rs16891982 (HERC2/OCA2), which contribute to reduced skin and eye pigmentation in Europeans,

dramatically increased in frequency during the Beaker and Bronze Age periods (Extended Data Fig. 5). Thus, the arrival of migrants associated with the Beaker Complex significantly altered the pigmentation phenotypes of British populations. However, the lactase persistence allele at SNP rs4988235 remained at very low frequencies in our dataset both in Britain and continental Europe, showing that the major increase in its frequency in Britain, as in mainland Europe, occurred in the last 3,500 years^{3,4,39,44}.

Discussion

The term “Bell Beaker” was introduced by late 19th-century and early 20th-century archaeologists to refer to the distinctive pottery style found across western and central Europe at the end of the Neolithic, initially hypothesized to have been spread by a genetically homogeneous group of people. This idea of a “Beaker Folk” became unpopular after the 1960s as scepticism about the role of migration in mediating change in archaeological cultures grew⁴⁵, although J.G.D. Clark speculated that the Beaker Complex expansion into Britain was an exception⁴⁶, a prediction that has now been borne out by ancient genomic data.

Our results clearly prove that the expansion of the Beaker Complex cannot be described by a simple one-to-one mapping of an archaeologically defined material culture to a genetically homogeneous population. This stands in contrast to other archaeological complexes analysed to date, notably the *Linearbandkeramik* first farmers of central Europe², the Yamnaya of the Pontic-Caspian Steppe^{2,3}, and to some extent the Corded Ware Complex of central and eastern Europe^{2,3}. Instead, our results support a model in which both cultural transmission and human migration played important roles, with the relative balance of these two processes depending on the region. In Iberia, the majority of Beaker Complex-associated individuals lacked Steppe affinities and were genetically most similar to preceding Iberian populations. In central Europe, Steppe ancestry was widespread and we can exclude a substantial contribution from Iberian Beaker Complex-associated individuals, contradicting initial suggestions of gene flow between these groups based on analysis of mtDNA⁴⁷ and dental morphology⁴⁸. Small-scale contacts remain plausible, however, as we observe small proportions of Steppe ancestry in two individuals from northern Spain.

Although cultural transmission seems to have been the main mechanism for the diffusion of the Beaker Complex between Iberia and central Europe, other parts of the Beaker Complex expansion were driven to a substantial extent by migration, with Beaker-associated burials in southern France, northern Italy, and Britain, representing the earliest occurrence of Steppe-related ancestry so far known in all three regions. This genomic transformation is clearest in Britain due to our dense genetic time transect. The earliest Beaker pots found in Britain show influences from both the lower Rhine region and the Atlantic façade of western Europe⁴⁹.

However, such dual influence is not mirrored in the genetic data, as the British Beaker Complex individuals were genetically most similar to lower Rhine individuals from the Netherlands. The arrival of the Beaker Complex precipitated a profound demographic transformation in Britain, exemplified by the absence of individuals in our dataset without large amounts of Steppe-related ancestry after 2400 BCE. It is possible that the uneven geographic distribution of our samples, coupled with different burial practises between local and incoming populations (cremation versus burial) during the early stages of interaction could result in a sampling bias against local individuals. However, the signal observed during the Beaker period persisted through the later Bronze Age, without any evidence of genetically Neolithic-like individuals among the 27 Bronze Age individuals we newly report, who traced more than 90% of their ancestry to individuals of the central European Beaker Complex. Thus, the genetic evidence points to a substantial amount of migration into Britain from the European mainland beginning around 2400 BCE. These results are notable in light of strontium and oxygen isotope analyses of British skeletons from the Beaker and Bronze Age periods⁵⁰, which have provided no evidence of substantial mobility over individuals' lifetimes from locations with cooler climates or from places with geologies atypical of Britain. However, the isotope data are only sensitive to first-generation migrants, and do not rule out movements from regions such as the lower Rhine, which is consistent with the genetic data, or from other geologically similar regions for which DNA sampling is still sparse. Further sampling of regions on the European continent may reveal additional candidate sources.

By analysing DNA data from ancient individuals we have been able to provide important constraints on the processes underlying cultural and social changes in Europe during the third millennium BCE. Our results raise new questions and motivate further archaeological research to identify the changes in social organization, technology, subsistence, climate, population sizes⁵¹ or pathogen exposure^{52,53} that could have precipitated the demographic changes uncovered in this study.

Methods

Ancient DNA analysis

We screened skeletal samples for DNA preservation in dedicated clean rooms. We extracted DNA^{54–56} and prepared barcoded next generation sequencing libraries, the majority of which were treated with uracil-DNA glycosylase to greatly reduce the damage (except at the terminal nucleotide) that is characteristic of ancient DNA^{57,58} (Supplementary Information, section 2). We initially enriched libraries for sequences overlapping the mitochondrial genome⁵⁹ and ~3000 nuclear SNPs using synthesized baits (CustomArray Inc.) that we PCR amplified. We sequenced the enriched material on an Illumina NextSeq instrument with 2x76 cycles, and 2x7 cycles to read out the two indices⁶⁰. We merged read pairs with the expected barcodes that overlapped by at least 15 base pairs, mapped the merged sequences to hg19 and to the reconstructed mitochondrial DNA consensus sequence⁶¹ using the *samse* command in bwa (v0.6.1)⁶², and removed duplicated sequences. We evaluated DNA authenticity by estimating the rate of mismatching to the consensus mitochondrial sequence⁶³, and also requiring that the rate of damage at the terminal nucleotide was at least 3% for UDG-treated libraries⁶³ and 10% for non-UDG-treated libraries⁶⁴.

For libraries that were promising after screening, we enriched in two consecutive rounds for sequences overlapping 1,233,013 SNPs ('1240k SNP capture')^{2,19} and sequenced 2x76 cycles and 2x7cycles on an Illumina NextSeq500 instrument. We processed the data bioinformatically as for the mitochondrial capture data, this time mapping only to the human reference genome *hg19* and merging the data from different libraries of the same individual. We further evaluated authenticity by studying the ratio of X-to-Y chromosome reads and estimating X-chromosome contamination in males based on the rate of heterozygosity⁶⁵. Samples with evidence of contamination were either filtered out or restricted to sequences with terminal cytosine deamination to remove sequences that could have derived from modern contaminants. Finally, we filtered out from our analysis dataset samples with fewer than 10,000 targeted SNPs covered at least once and samples that were first-degree relatives of others in the dataset (keeping the sample with the larger number of covered SNPs) (Supplementary Table 1).

Mitochondrial haplogroup determination

We used the mitochondrial capture bam files to determine the mitochondrial haplogroup of each sample with new data, restricting to reads with MAPQ \geq 30 and base quality \geq 30. First, we constructed a consensus sequence with samtools and bcftools⁶⁶, using a majority rule and requiring a minimum coverage of 2. We called haplogroups with HaploGrep2⁶⁷ based on

phylotree⁶⁸ (mtDNA tree Build 17 (18 Feb 2016)). Mutational differences compared to the rCRS and corresponding haplogroups can be viewed in Supplementary Table 2.

Y-chromosome analysis

We determined Y-chromosome haplogroups for both new and published samples (Supplementary Information, section 3). We made use of the sequences mapping to 1240k Y-chromosome targets, restricting to sequences with mapping quality ≥ 30 and bases with quality ≥ 30 . We called haplogroups by determining the most derived mutation for each sample, using the nomenclature of the International Society of Genetic Genealogy (<http://www.isogg.org>) version 11.110 (21 April 2016). Haplogroups and their supporting derived mutations can be viewed in Supplementary Table 3.

Merging newly generated data with published data

We assembled two datasets for population genetics analyses:

- *HO* includes 2,572 present-day individuals from worldwide populations genotyped on the Human Origins Array^{22,31,69} and 470 ancient individuals. The ancient set includes 103 Beaker Complex individuals (87 newly reported, 5 with shotgun data³ for which we generated 1240k capture data and 11 previously published^{3,4}), 68 newly reported individuals from relevant ancient populations and 298 previously published^{2-4,20-37} individuals (Supplementary Table 1). We kept 591,642 autosomal SNPs after intersecting autosomal SNPs in the 1240k capture with the analysis set of 594,924 SNPs from Lazaridis et al.²².

- *HOIII* includes the same set of ancient samples and 300 present-day individuals from 142 populations sequenced to high coverage as part of the Simons Genome Diversity Project³⁸. For this dataset, 1,054,671 autosomal SNPs were used, excluding SNPs of the 1240k array located on sex chromosomes or with known functional effects.

For both datasets, ancient individuals were merged by randomly sampling one read at each SNP position, discarding the first and the last two nucleotides of each read.

Principal component analysis

We carried out principal component analysis (PCA) on the *HO* dataset using the *smartpca* program in EIGENSOFT⁷⁰. We computed principal components on 990 present-day West Eurasians and projected ancient individuals using lsqproject: YES and shrinkmode: YES.

ADMIXTURE analysis

We performed model-based clustering analysis using ADMIXTURE⁴¹ on the *HO* reference dataset, including 2,572 present-day individuals from worldwide populations and the ancient individuals. First, we carried out LD-pruning on the dataset using PLINK⁷¹ with the flag --indep-pairwise 200 25 0.4, keeping 306,393 SNPs. We ran ADMIXTURE with the cross validation (--cv) flag specifying from K=2 to K=20 clusters, with 20 replicates for each value of K and keeping for each value of K the replicate with highest log likelihood. In Extended Data Fig. 1b we show the cluster assignments at K=8 of newly reported individuals and other relevant ancient samples for comparison. This value of K was the lowest for which components of Caucasus hunter-gatherers (CHG) and European hunter-gatherers were maximized.

f-statistics

We computed *f*-statistics on the *HOIII* dataset using ADMIXTOOLS⁶⁹ with default parameters (Supplementary Information, section 4). We used *qpDstat* with f4mode:Yes for *f*₄-statistics and *qp3Pop* for outgroup *f*₃-statistics. We computed standard errors using a weighted block jackknife⁷² over 5 Mb blocks.

Inference of mixture proportions

We estimated ancestry proportions on the *HOIII* dataset using *qpAdm*² and a basic set of 9 *Outgroups*: Mota, Ust_Ishim, MA1, Villabruna, Mbuti, Papuan, Onge, Han, Karitiana. For some analyses (Supplementary Information, section 6) we added additional outgroups to this basic set.

Allele frequency estimation from read counts

We used allele counts at each SNP to perform maximum likelihood estimation of allele frequencies in ancient populations as in ref.⁴. In Extended Data Fig. 5, we show derived allele frequency estimates at three SNPs of functional importance for different ancient populations.

Data availability

All 1240k and mitochondrial capture sequencing data is available from the European Nucleotide Archive, accession number XXXXXXXXX [to be made available on publication].
Pseudo haploid genotype data is available from the Reich Lab website at [to be made available on publication].

Acknowledgements

We thank D. Anthony, J. Koch, I. Mathieson and C. Renfrew for comments and critiques. We thank A. C. Sousa for providing geographical information on a Portuguese sample and A. Martín and L. Loe for help in contacting archaeologists. We thank M. Giesen for assisting with samples selection. We thank the Museo Arqueológico Regional de la Comunidad de Madrid for kindly allowing access to samples from Camino de las Yeseras. We thank the Hunterian Museum, University of Glasgow, for allowing access to samples from sites in Scotland, and particularly to Dr. S.-A. Coupar for help in accessing material. We thank the Museu Municipal de Torres Vedras for allowing the study and sampling of Cova da Moura collection. We are grateful to the Orkney Museum for allowing access to samples from Orkney, and particularly to G. Drinkall for facilitating this work. We thank the Great North Museum: Hancock, the Society of Antiquaries of Newcastle upon Tyne, and Sunderland Museum for sharing samples. We are grateful to E. Willerslev for sharing several dozen samples that were analyzed in this study and for supporting several co-authors at the Centre for GeoGenetics at the University of Copenhagen who worked on this project. We are grateful for institutional support (grant RVO:67985912) from the Institute of Archaeology, Czech Academy of Sciences. G.K. was supported by Momentum Mobility Research Group of the Hungarian Academy of Sciences. This work was supported by the Wellcome Trust [100713/Z/12/Z]. D.F. was supported by an Irish Research Council grant GOIPG/2013/36. P.W.S., J.K. and A.M. were supported by the Heidelberg Academy of Sciences (WIN project “Times of Upheaval”). C.L.-F. was supported by a grant from FEDER and Ministry of Economy and Competitiveness (BFU2015-64699-P) of Spain. D.R. was supported by US National Science Foundation HOMINID grant BCS-1032255, US National Institutes of Health grant GM100233, and is an investigator of the Howard Hughes Medical Institute.

Author Contributions

S.B., M.E.A, N.R., A.S.-N., A.M., N.B., M.F., E.H., M.M., J.O., K.S., R.P., J.K., W.H., I.B. and D.R. performed or supervised wet laboratory work. G.T.C. undertook the radiocarbon dating of a large fraction of the British samples. I.A., K.K., A.B., K.W.A., A.A.F., E.B., M.B.-B., D.B., C.B., C.Bo., L.B., T.A., L.Bü., S.C., L.C.N., O.E.C., G.C., B.C., A.D., K.E.D., N.D., M.E.,

462 C.E., M.K., J.F.F., H.F., C.F., M.G., R.G.P., M.H.-U., E.Had., G.H., N.J., T.K., K.M., S.P.,
 463 P.L., O.L., A.L., J.L.M., T.M., J.I.M, K.Mc., M.B.G., A.Mo., G.K., V.K., A.C., R.Pa., A.E.,
 464 K.Kö., T.H., J.L.C., C.L., M.P.P., P.W., T.D.P., P.P., P.-J.R., P.R., R.R., M.A.R.G., A.S., J.S.,
 465 A.M.S., V.S., L.V., J.Z., D.C., T.Hi., V.H., A.Sh., K.-G.S., P.W.S., R.P., J.K., W.H., I.B., C.L.-
 466 F. and D.R. assembled archaeological material. I.O., S.M., T.B., A.M., E.A., M.L., I.L., N.P.,
 467 Y.D., Z.F., D.F., P.d.K., M.G.T. and D.R. analysed or supervised analysis of data. I.O., C.L.-F.
 468 and D. R. wrote the manuscript with input from all co-authors.

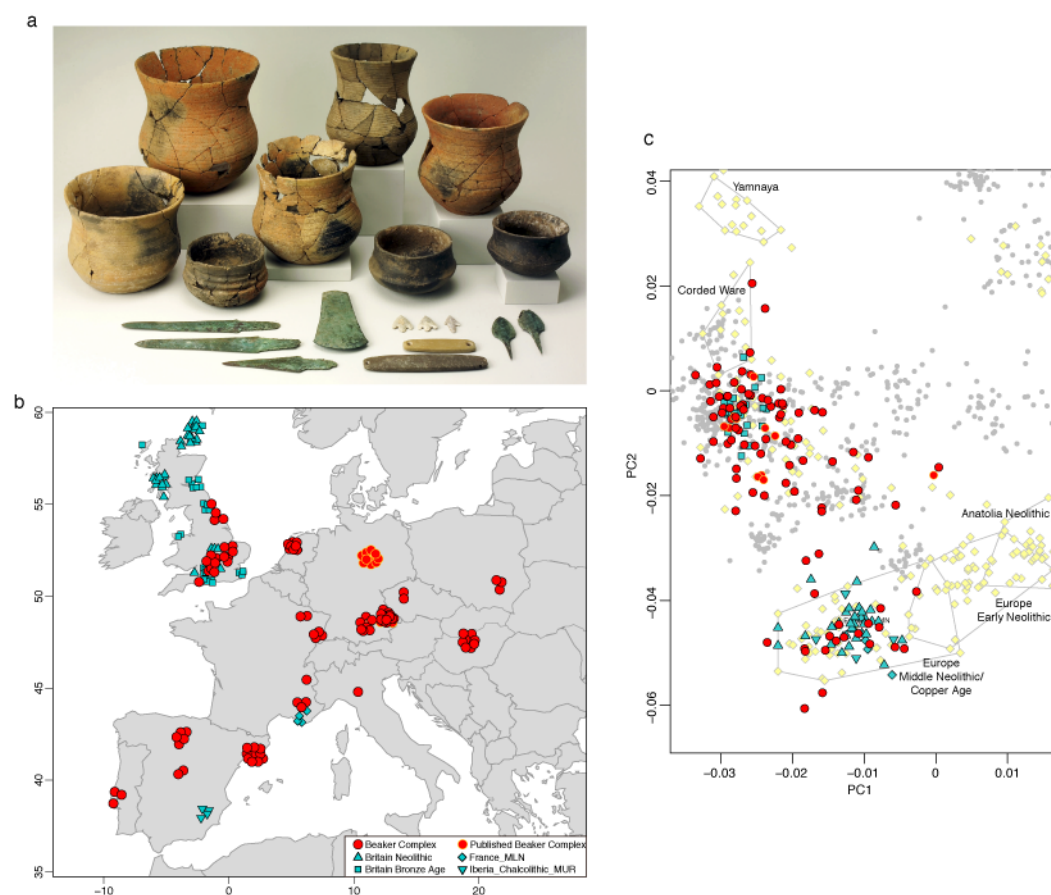


Figure 1. Genetic structure of individuals included in this study. **a**, Beaker Complex grave goods from La Sima III barrow⁷³. Photo: Alejandro Plaza, Museo Numantino. **b**, Geographic distribution of samples with new genome-wide data, with random jitter added for clarity. **c**, Principal component analysis of 990 present-day West Eurasian individuals (grey dots), with previously published (pale yellow) and new ancient samples projected onto the first two principal components. This figure is a zoom of Extended Data Fig 1a.

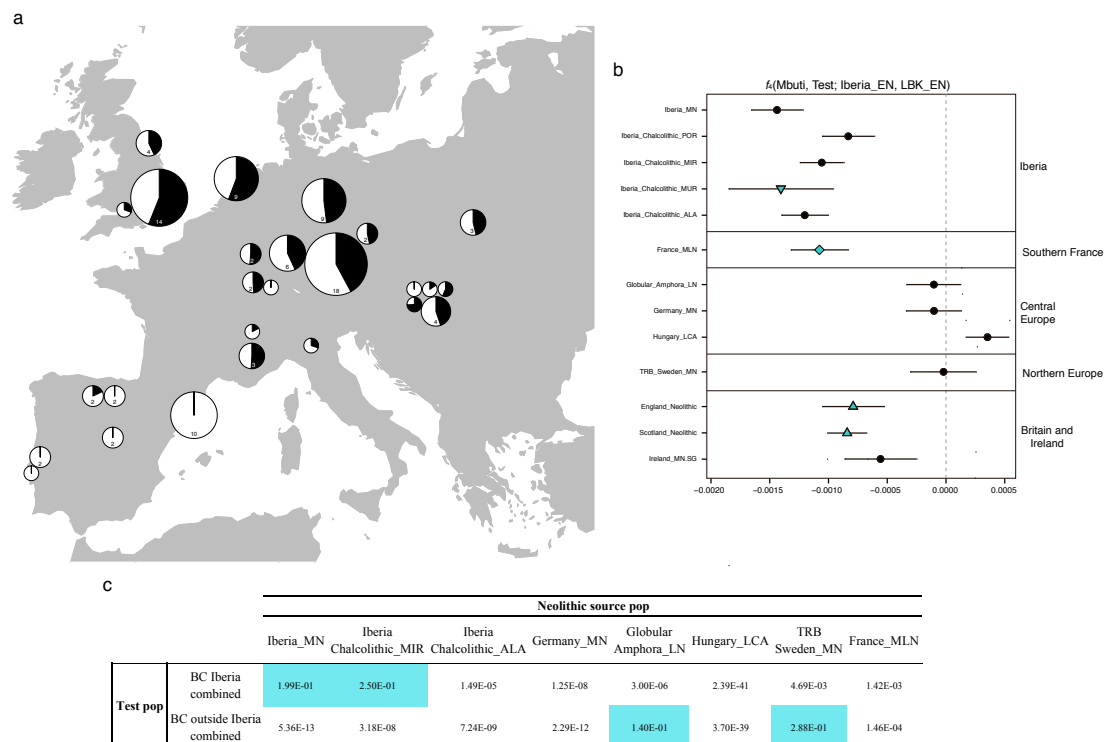


Figure 2. Investigating the genetic makeup of Beaker Complex individuals. **a**, Proportion of Steppe-related ancestry (shown in black) in Beaker Complex groups, computed with *qpAdm* under the model Yamnaya_Samara + Anatolia_Neolithic + WHG. The area of the pie is proportional to the number of individuals (shown inside the pie if more than one). See Supplementary Information, section 6 for mixture proportions and standard errors. **b**, f_4 -statistics of the form $f_4(\text{Mbuti}, \text{Test}; \text{Iberia_EN}, \text{LBK_EN})$ computed for European populations before the emergence of the Beaker Complex. Error bars represent ± 1 standard errors. **c**, Testing different populations as a source for the Neolithic farmer ancestry component in Beaker Complex individuals. The table shows the P-values (highlighted if > 0.05) for the model: Yamnaya_Samara + Neolithic farmer population. BC, Beaker complex.

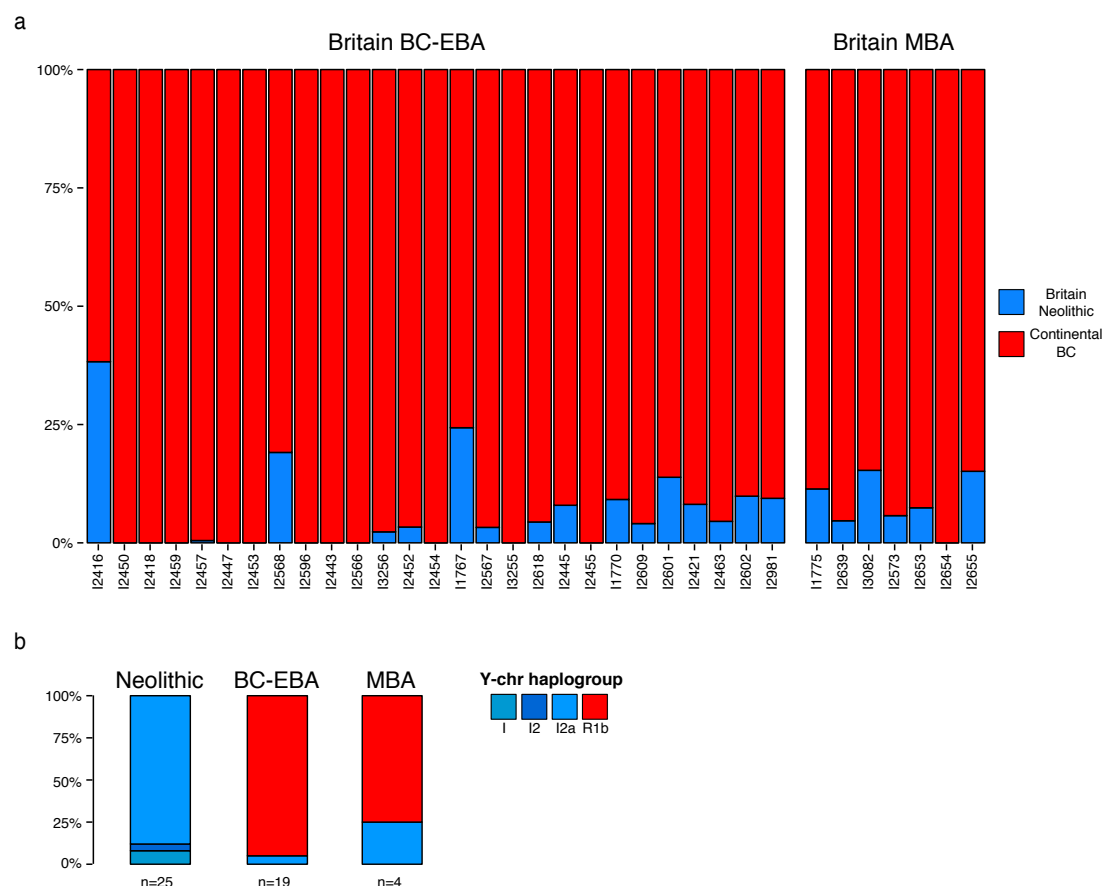


Figure 3. Population transformation in Britain associated with the arrival of the Beaker Complex. **a**, Modelling Beaker Complex and Bronze Age individuals from Britain as a mixture of continental Beaker Complex (red, represented by Beaker Complex samples from Oostwoud) and Britain_Neolithic (blue). Individuals are ordered chronologically (oldest on the left) and included in the plot if represented by more than 100,000 SNPs. See Supplementary Information, section 6 for mixture proportions and standard errors. **b**, Y-chromosome haplogroup distribution in males from Britain. EBA, Early Bronze Age; MBA, Middle Bronze Age. BC, Beaker complex.

Supplementary Tables

Supplementary Table 1. Ancient individuals included in this study.

Supplementary Table 2. Mitochondrial haplogroup calls for individuals with newly reported data.

Supplementary Table 3. Y-chromosome calls for males with newly reported data .

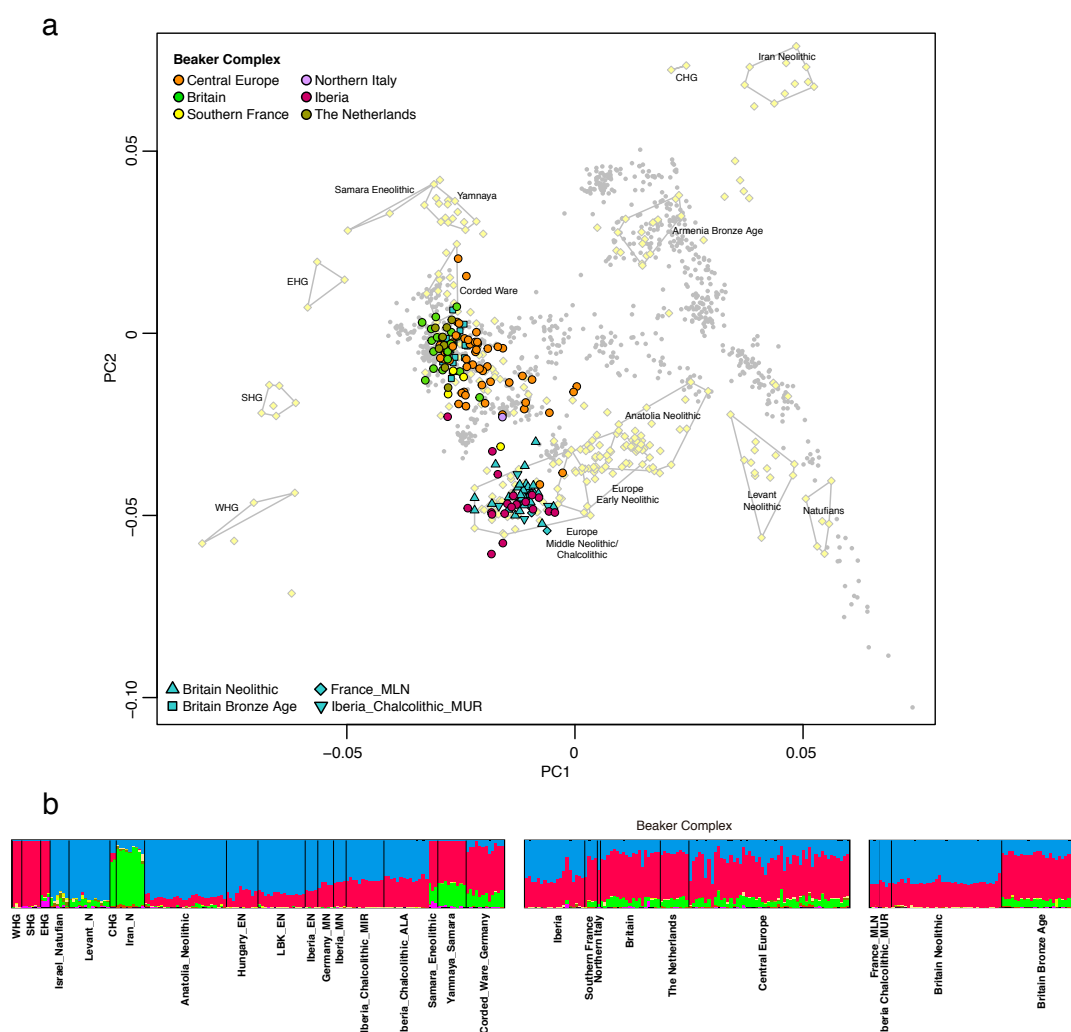
References

1. Czebreszuk, J. Bell Beakers from West to East. In *Ancient Europe, 8000 B.C. to A.D. 1000: An Encyclopedia of the Barbarian World* (eds. Bogucki, P. I. & Crabtree, P. J.) 476–485 (Charles Scribner's Sons, 2004).
2. Haak, W. *et al.* Massive migration from the steppe was a source for Indo-European languages in Europe. *Nature* **522**, 207–211 (2015).
3. Allentoft, M. E. *et al.* Population genomics of Bronze Age Eurasia. *Nature* **522**, 167–172 (2015).
4. Mathieson, I. *et al.* Genome-wide patterns of selection in 230 ancient Eurasians. *Nature* **528**, 499–503 (2015).
5. Cardoso, J. L. Absolute chronology of the Beaker phenomenon North of the Tagus estuary : demographic and social implications. *Trab. Prehist.* **71**, 56–75 (2014).
6. Müller, J. & van Willigen, S. New radiocarbon evidence for European Bell Beakers and the consequences for the diffusion of the Bell Beaker phenomenon. In *Bell beakers today: pottery, people, culture, symbols in prehistoric Europe. proceedings of the International colloquium, Riva del Garda (Trento, Italy)* (ed. Nicolis, F.) 59–80 (2001).
7. Jeunesse, C. The dogma of the Iberian origin of the Bell Beaker: attempting its deconstruction. *J. Neolit. Archaeol.* **16**, 158–166 (2015).
8. Rojo Guerra, M., Garrido-Pena, R. & García-Martínez de Lagrán, Í. *Bell Beakers in the Iberian Peninsula and their european context*. (Universidad de Valladolid, 2005).
9. Czebreszuk, J. *Similar But Different. Bell Beakers in Europe*. (Sidestone Press, 2004).
10. Harrison, R. & Heyd, V. The Transformation of Europe in the Third Millennium BC: the example of 'Le Petit-Chasseur I + III' (Sion, Valais, Switzerland). In *Praehistorische Zeitschrift* **82**, (2007).
11. Lemerrier, O. Historical model of setting and spreading out of the Bell Beaker culture in Mediterranean France. In *Similar But Different: Bell Beakers in Europe* (ed. Czebreszuk, J.) 193–205 (2004).
12. Bailly, M. & Salanova, L. Les dates radiocarbones du Campaniforme en Europe Occidentale : Analyse critique des principales séries de dates. *Mémoires la Société préhistorique française* **26**, 219–224 (1999).
13. Prieto-Martínez, M. P. Perceiving changes in the third millennium BC in Europe through pottery: Galicia, Brittany and Denmark as examples. In *Becoming European: The transformation of third millennium northern and western Europe* (eds. Prescott, C. & Glorstad, H.) 30–47 (Oxford: Oxbow Books, 2011).
14. Fokkens, H. & Nicolis, F. *Background to Beakers. Inquiries into regional cultural backgrounds of the Bell Beaker complex*. (Leiden: Sidestone Press, 2012).
15. Grupe, G. *et al.* Mobility of Bell Beaker people revealed by strontium isotope ratios of tooth and bone: a study of southern Bavarian skeletal remains. *Appl. Geochemistry* **12**, 517–525 (1997).
16. Price, T. D., Knipper, C., Grupe, G. & Smrcka, V. Strontium Isotopes and Prehistoric Human Migration: The Bell Beaker Period in Central Europe. *Eur. J. Archaeol.* **7**, 9–40 (2004).
17. Vander Linden, M. What linked the Bell Beakers in third millennium BC Europe? *Antiquity* **81**, 343–352 (2007).

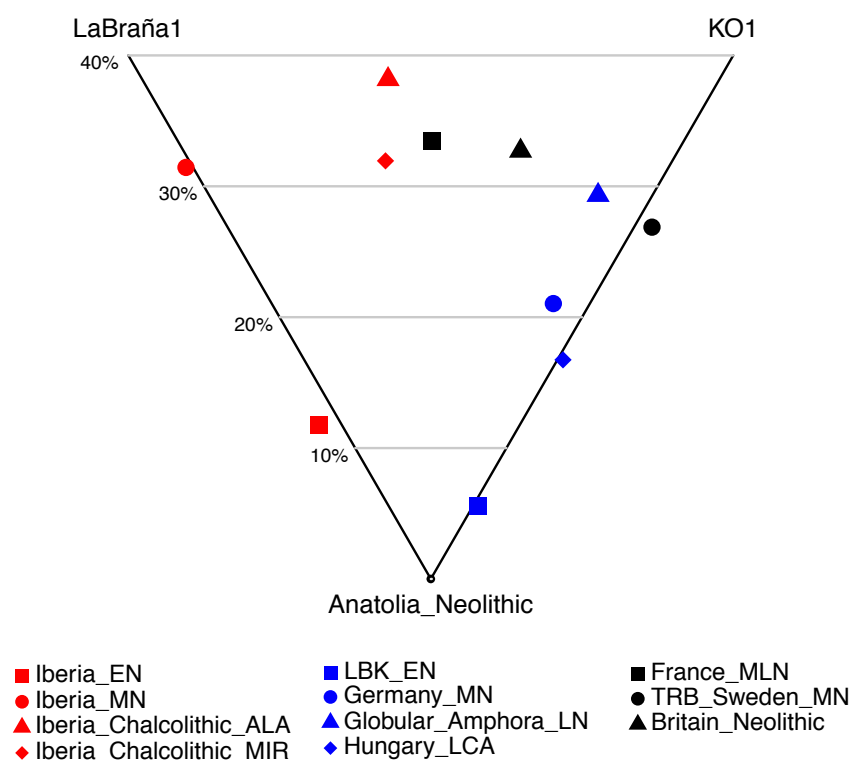
18. Lemerrier, O. Interpreting the Beaker phenomenon in Mediterranean France: an Iron Age analogy. *Antiquity* **86**, 131–143 (2012).
19. Fu, Q. *et al.* An early modern human from Romania with a recent Neanderthal ancestor. *Nature* **524**, 216–219 (2015).
20. Keller, A. *et al.* New insights into the Tyrolean Iceman's origin and phenotype as inferred by whole-genome sequencing. *Nat. Commun.* **3**, 698 (2012).
21. Raghavan, M. *et al.* Upper Palaeolithic Siberian genome reveals dual ancestry of Native Americans. *Nature* **505**, 87–91 (2014).
22. Lazaridis, I. *et al.* Ancient human genomes suggest three ancestral populations for present-day Europeans. *Nature* **513**, 409–413 (2014).
23. Seguin-Orlando, A. *et al.* Genomic structure in Europeans dating back at least 36,200 years. *Science* **346**, 1113–1118 (2014).
24. Fu, Q. *et al.* Genome sequence of a 45,000-year-old modern human from western Siberia. *Nature* **514**, 445–449 (2014).
25. Olalde, I. *et al.* A Common Genetic Origin for Early Farmers from Mediterranean Cardial and Central European LBK Cultures. *Mol. Biol. Evol.* **32**, 3132–3142 (2015).
26. Günther, T. *et al.* Ancient genomes link early farmers from Atapuerca in Spain to modern-day Basques. *Proc. Natl. Acad. Sci. U. S. A.* **112**, 11917–11922 (2015).
27. Jones, E. R. *et al.* Upper palaeolithic genomes reveal deep roots of modern eurasians. *Nat. Comm.* **6**, 1–8 (2015).
28. Cassidy, L. M. *et al.* Neolithic and Bronze Age migration to Ireland and establishment of the insular Atlantic genome. *Proc. Natl. Acad. Sci. U. S. A.* **113**, 1–6 (2016).
29. Gallego Llorente, M. *et al.* Ancient Ethiopian genome reveals extensive Eurasian admixture in Eastern Africa. *Science* **350**, 820–822 (2015).
30. Fu, Q. *et al.* The genetic history of Ice Age Europe. *Nature* **534**, 200–205 (2016).
31. Lazaridis, I. *et al.* Genomic insights into the origin of farming in the ancient Near East. *Nature* **536**, 1–22 (2016).
32. Skoglund, P. *et al.* Genomic Diversity and Admixture Differs for Stone-Age Scandinavian Foragers and Farmers. *Science* **201**, 786–792 (2014).
33. Kilinc, G. M. *et al.* The Demographic Development of the First Farmers in Anatolia. *Curr. Biol.* **26**, 1–8 (2016).
34. Gallego-Llorente, M. *et al.* The genetics of an early Neolithic pastoralist from the Zagros, Iran. *Sci. Rep.* **6**, 4–10 (2016).
35. Broushaki, F. *et al.* Early Neolithic genomes from the eastern Fertile Crescent. *Science* **7943**, 1–16 (2016).
36. Olalde, I. *et al.* Derived immune and ancestral pigmentation alleles in a 7,000-year-old Mesolithic European. *Nature* **507**, 225–8 (2014).
37. Hofmanová, Z. *et al.* Early farmers from across Europe directly descended from Neolithic Aegeans. *Proc. Natl. Acad. Sci. U. S. A.* **113**, 6886–6891 (2016).
38. Mallick, S. *et al.* The Simons Genome Diversity Project: 300 genomes from 142 diverse populations. *Nature* **538**, (2016).
39. Gamba, C. *et al.* Genome flux and stasis in a five millennium transect of European prehistory. *Nat. Commun.* **5**, 5257 (2014).
40. Valverde, L. *et al.* New clues to the evolutionary history of the main European paternal lineage M269: dissection of the Y-SNP S116 in Atlantic Europe and Iberia. *Eur. J. Hum. Genet.* 1–5 (2015). doi:10.1038/ejhg.2015.114
41. Alexander, D. H., Novembre, J. & Lange, K. Fast model-based estimation of ancestry in unrelated individuals. *Genome Res.* **19**, 1655–1664 (2009).
42. Lipson, M. *et al.* Parallel ancient genomic transects reveal complex population history of early European farmers. *bioRxiv* (2017).
43. Sheridan, J. A. The Neolithisation of Britain and Ireland: the big picture. In *Landscapes in transition* (eds. Finlayson, B. & Warren, G.) 89–105 (Oxbow, Oxford, 2010).
44. Burger, J., Kirchner, M., Bramanti, B., Haak, W. & Thomas, M. G. Absence of the lactase-persistence-associated allele in early Neolithic Europeans. *Proc. Natl. Acad. Sci. U. S. A.* **104**, 3736–41 (2007).

45. Clarke, D. L. The Beaker network: social and economic models. In *Glockenbecher Symposion, Oberried, 18–23 März 1974* (eds. Lanting, J. N. & DerWaals, J. D. van) 460–77 (1976).
46. Clark, G. The Invasion Hypothesis in British Archaeology. *Antiquity* **40**, 172–189 (1966).
47. Brotherton, P. *et al.* Neolithic mitochondrial haplogroup H genomes and the genetic origins of Europeans. *Nat. Commun.* **4**, 1764 (2013).
48. Desideri, J. When Beakers Met Bell Beakers: an analysis of dental remains. *British archaeological Reports - International Series*; 2292 (2011).
49. Needham, S. Transforming Beaker Culture in North-West Europe; Processes of Fusion and Fission. *Proc. Prehist. Soc.* **71**, 171–217 (2005).
50. Parker Pearson, M. *et al.* Beaker people in Britain: migration, mobility and diet. *Antiquity* **90**, 620–637 (2016).
51. Shennan, S. *et al.* Regional population collapse followed initial agriculture booms in mid-Holocene Europe. *Nat. Commun.* **4**, 2486 (2013).
52. Valtueña, A. A. *et al.* The Stone Age Plague: 1000 years of Persistence in Eurasia. *bioRxiv* (2016).
53. Rasmussen, S. *et al.* Early Divergent Strains of *Yersinia pestis* in Eurasia 5,000 Years Ago. *Cell* **163**, 571–582 (2015).
54. Dabney, J. *et al.* Complete mitochondrial genome sequence of a Middle Pleistocene cave bear reconstructed from ultrashort DNA fragments. *Proc. Natl. Acad. Sci. U. S. A.* **110**, 15758–63 (2013).
55. Damgaard, P. B. *et al.* Improving access to endogenous DNA in ancient bones and teeth. *Sci. Rep.* **5**, 11184 (2015).
56. Korlević, P. *et al.* Reducing microbial and human contamination in dna extractions from ancient bones and teeth. *Biotechniques* **59**, 87–93 (2015).
57. Rohland, N., Harney, E., Mallick, S., Nordenfelt, S. & Reich, D. Partial uracil – DNA – glycosylase treatment for screening of ancient DNA. *Philos. Trans. R. Soc. London B* (2015). doi:10.1098/rstb.2013.0624
58. Briggs, A. W. *et al.* Removal of deaminated cytosines and detection of in vivo methylation in ancient DNA. *Nucleic Acids Res.* **38**, 1–12 (2010).
59. Maricic, T., Whitten, M. & Pääbo, S. Multiplexed DNA sequence capture of mitochondrial genomes using PCR products. *PLoS One* **5**, e14004 (2010).
60. Kircher, M., Sawyer, S. & Meyer, M. Double indexing overcomes inaccuracies in multiplex sequencing on the Illumina platform. *Nucleic Acids Res.* **40**, 1–8 (2012).
61. Behar, D. M. *et al.* A ‘Copernican’ reassessment of the human mitochondrial DNA tree from its root. *Am. J. Hum. Genet.* **90**, 675–84 (2012).
62. Li, H. & Durbin, R. Fast and accurate short read alignment with Burrows–Wheeler transform. *Bioinformatics* **25**, 1754–1760 (2009).
63. Fu, Q. *et al.* A revised timescale for human evolution based on ancient mitochondrial genomes. *Curr. Biol.* **23**, 553–9 (2013).
64. Sawyer, S., Krause, J., Guschanski, K., Savolainen, V. & Pääbo, S. Temporal patterns of nucleotide misincorporations and DNA fragmentation in ancient DNA. *PLoS One* **7**, e34131 (2012).
65. Korneliussen, T. S., Albrechtsen, A. & Nielsen, R. ANGSD: Analysis of Next Generation Sequencing Data. *BMC Bioinformatics* **15**, 1–13 (2014).
66. Li, H. *et al.* The Sequence Alignment/Map format and SAMtools. *Bioinformatics* **25**, 2078–9 (2009).
67. Weissensteiner, H. *et al.* HaploGrep 2: mitochondrial haplogroup classification in the era of high-throughput sequencing. *Nucleic Acids Res.* **44**, W58–63 (2016).
68. van Oven, M. & Kayser, M. Updated comprehensive phylogenetic tree of global human mitochondrial DNA variation. *Hum. Mutat.* **30**, E386–94 (2009).
69. Patterson, N. *et al.* Ancient admixture in human history. *Genetics* **192**, 1065–93 (2012).
70. Patterson, N., Price, A. L. & Reich, D. Population structure and eigenanalysis. *PLoS Genet.* **2**, e190 (2006).

71. Purcell, S. *et al.* PLINK : A Tool Set for Whole-Genome Association and Population-Based Linkage Analyses. *Am. J. Hum. Genet.* **81**, 559–575 (2007).
72. Busing, F. M. T. A., Meijer, E. & Van Der Leeden, R. Delete- m Jackknife for Unequal m. *Stat. Comput.* **9**, 3–8 (1999).
73. Busing, F. M. T. A., Meijer, E. & Van Der Leeden, R. Delete- m Jackknife for Unequal m. *Stat. Comput.* **9**, 3–8 (1999).
74. Rojo-Guerra, M. Á., Kunst, M., Garrido-Pena, R. & García-Martínez de Lagrán, I. Morán-Dauchez, G. Un desafío a la eternidad. Tumbas monumentales del Valle de Ambrona. Memorias Arqueología en Castilla y León 14, Junta de Castilla y León, Valladolid (2005).

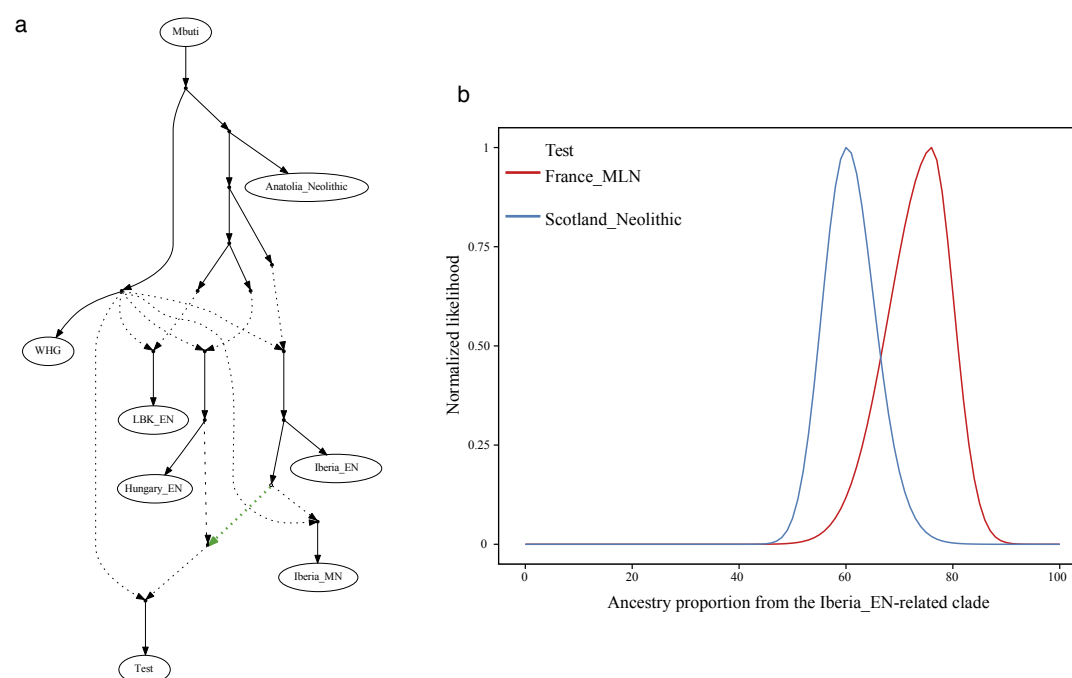


Extended Data Figure 1. Population structure. **a**, Principal component analysis of 990 present-day West Eurasian individuals (grey dots), with previously published (pale yellow) and new ancient samples projected onto the first two principal components. **b**, ADMIXTURE clustering analysis with $k=8$ showing ancient individuals. E/M/MLN, Early/Middle/Middle Late Neolithic; W/E/S/CHG, Western/Eastern/Scandinavian/Caucasus hunter-gatherers.

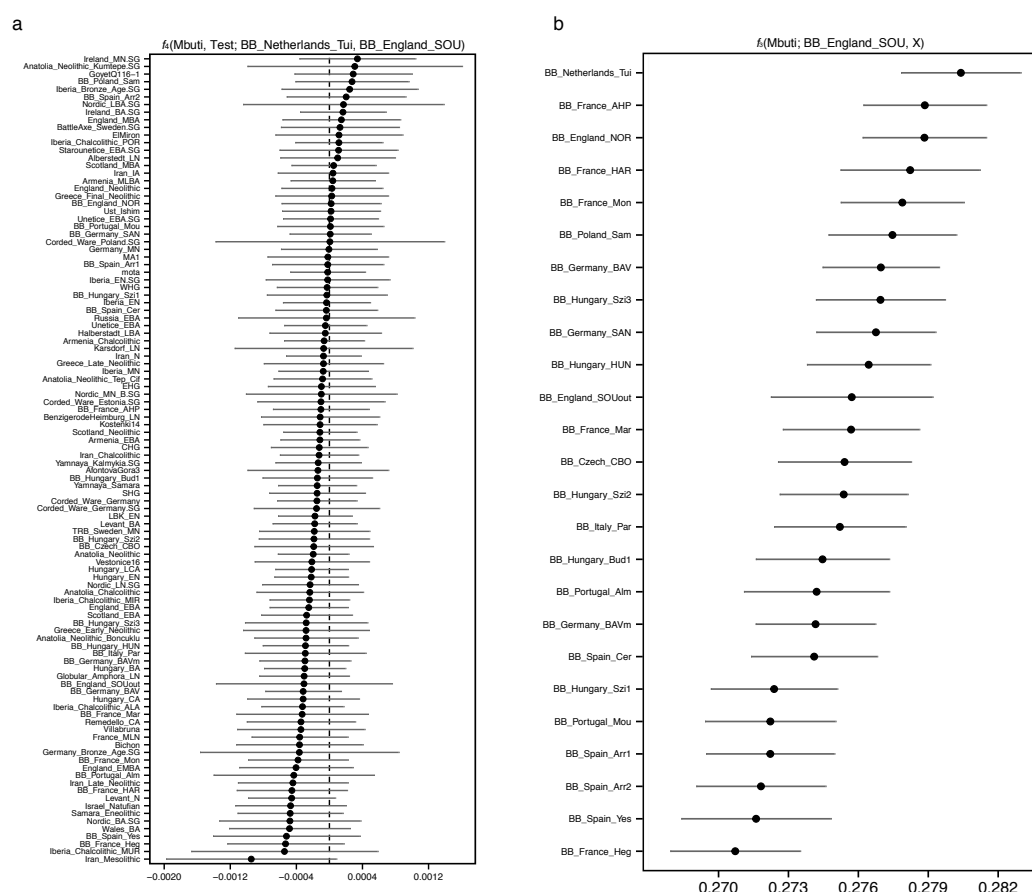


Extended Data Figure 2. Hunter-gatherer affinities in Neolithic/Copper Age Europe.

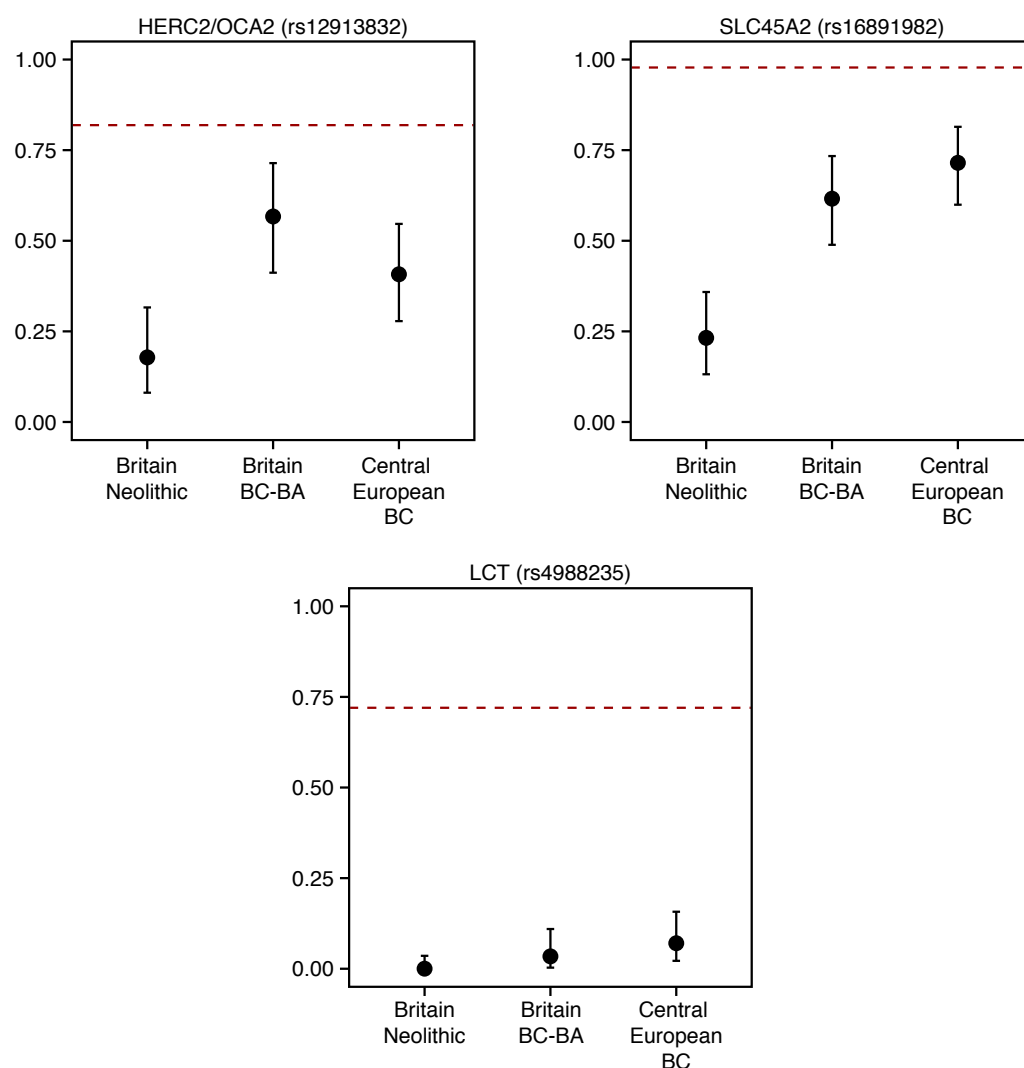
Differential affinity to hunter-gatherer individuals (LaBraña1³⁶ from Spain and KO1³⁹ from Hungary) in European populations before the emergence of the Beaker Complex. See Supplementary Information, section 6 for mixture proportions and standard errors computed with *qpAdm*.



Extended Data Figure 3. Modelling the relationships between Neolithic populations. a, Admixture graph fitting a *Test* population as a mixture of sources related to both Iberia_EN and Hungary_EN. **b,** Likelihood distribution for models with different proportions of the source related to Iberia_EN (green admixture edge in (a)) when *Test* is Great Britain_Neolithic or France_MLN.



Extended Data Figure 4. Genetic affinity between Beaker complex individuals from southern Great Britain and the Netherlands. **a**, f_4 -statistics of the form $f_4(\text{Mbuti, Test; BB_Netherlands_Tui, BB_Great Britain_SOU})$. Negative values indicate that Test is closer to BB_Netherlands_Tui than to BB_Great Britain_SOU, and the opposite for positive values. Error bars represent ± 3 standard errors. **b**, Outgroup- f_3 statistics of the form $f_3(\text{Mbuti; BB_Great Britain_SOU, X})$ measuring shared genetic drift between BB_Great Britain_SOU and other Beaker Complex groups. Error bars represent ± 1 standard errors.



Extended Data Figure 5. Derived allele frequencies at three SNPs of functional importance. Error bars represent 1.9-log-likelihood support interval. The red dashed lines show allele frequencies in the 1000 Genomes GBR population (present-day people from Great Britain). BC, Beaker Complex; BA, Bronze Age.

Extended Data Table 1. 62 Newly reported radiocarbon dates

Sample	Date	Location	Country
I4145	2279–2033 calBCE (3740±35 BP, Poz-84460)	Kněževes	Czech Republic
I1392	2832–2476 calBCE (4047±29 BP, MAMS-25935)	Hégenheim Necropole, Haut-Rhin	France
I4144	2572–2512 calBCE (3955±35 BP, Poz-84553)	Osterhofen-Altenmarkt	Germany
E09537_d	2471–2300 calBCE (3909±29 BP, MAMS 29074)	Unterer Talweg 58-62, Augsburg, Bavaria	Germany
I4249	2336–2141 calBCE (3802±26 BP, BRAMS1217)	Irlbach LKR	Germany
E09538	2464–2212 calBCE (3870±30 BP, MAMS 29075)	Unterer Talweg 58-62, Augsburg, Bavaria	Germany
I3592	2458–2204 calBCE (3844±33 BP, BRAMS-1218)	Alburg-Lerchenhaid, Spedition Häring, Bavaria	Germany
I4250	2434–2150 calBCE (3825±26 BP, BRAMS1219)	Irlbach LKR	Germany
I3593	2398–2146 calBCE (3817±26 BP, BRAMS-1215)	Alburg-Lerchenhaid, Spedition Häring, Bavaria	Germany
I3590	2339–2143 calBCE (3802±26 BP, BRAMS-1217)	Alburg-Lerchenhaid, Spedition Häring, Bavaria	Germany
I2657	3952–3781 calBCE (5052±30 BP, SUERC-68701)	Macarthur Cave	Great Britain
I2633	3766–3642 calBCE (4911±32 BP, SUERC-68634)	Tulloch of Assery B	Great Britain
I2659	3762–3644 calBCE (4914±27 BP, SUERC-68702)	Distillery Cave	Great Britain
I2691	3701–3640 calBCE (4881±25 BP, SUERC-68704)	Distillery Cave	Great Britain
I2796	3706–3536 calBCE (4856±33 BP, SUERC-69074)	Point of Cott, Orkney	Great Britain
I2634	3704–3535 calBCE (4851±34 BP, SUERC-68638)	Tulach an t'Sionnach	Great Britain
I2635	3653–3390 calBCE (4796±37 BP, SUERC-68639)	Tulloch of Assery A	Great Britain
I2636	3520–3362 calBCE (4651±33 BP, SUERC-68640)	Holm of Papa Westray North	Great Britain
I2988	3517–3362 calBCE (4645±29 BP, SUERC-68711)	Clachaig	Great Britain
I2660	3514–3353 calBCE (4631±29 BP, SUERC-68703)	Distillery Cave	Great Britain
I2650	3500–3360 calBCE (4754±36 BP, SUERC-68642)	Holm of Papa Westray North	Great Britain
I2637	3510–3340 calBCE (4697±33 BP, SUERC-68641)	Holm of Papa Westray North	Great Britain
I2605	3632–3373 calBCE (4710±35 BP, Poz-83483)	Eton Rowing Course	Great Britain
I2980	3361–3102 calBCE (4530±33 BP, SUERC-69073)	Point of Cott, Orkney	Great Britain
I2651	3330–3090 calBCE (4525±36 BP, SUERC-68643)	Holm of Papa Westray North	Great Britain
I3085	3339–3027 calBCE (4471±29 BP, SUERC-68724)	Isbister, Orkney	Great Britain
I2978	3336–3024 calBCE (4464±29 BP, SUERC-68725)	Isbister, Orkney	Great Britain
I2934	3327–3036 calBCE (4466±33 BP, SUERC-69071)	Isbister, Orkney	Great Britain
I2935	3336–3012 calBCE (4451±29 BP, SUERC-68723)	Isbister, Orkney	Great Britain
I2979	3334–2942 calBCE (4447±29 BP, SUERC-68726)	Isbister, Orkney	Great Britain
I2631	3098–2907 calBCE (4384±36 BP, SUERC-68633)	Quoyness	Great Britain
I2933	3011–2886 calBCE (4309±29 BP, SUERC-68722)	Isbister, Orkney	Great Britain
I2977	3009–2764 calBCE (4275±33 BP, SUERC-69072)	Isbister, Orkney	Great Britain
I2630	2581–2464 calBCE (3999±32 BP, SUERC-68632)	Isbister, Orkney	Great Britain
I2932	2571–2348 calBCE (3962±29 BP, SUERC-68721)	Isbister, Orkney	Great Britain
I2612	2465–2209 calBCE (3865±35 BP, Poz-83492)	Hasting Hill, Sunderland, Tyne and Wear	Great Britain
I2416	2470–2285 calBC (3830±30 BP, Beta-432804)	Amesbury Down, Wiltshire	Great Britain
I2418	2440–2200 calBCE (3835±25 BP, NZA-32788)	Amesbury Down, Wiltshire	Great Britain
I2565	2470–2140 calBCE (3829±38 BP, OxA-13562)	Amesbury Down, Wiltshire	Great Britain
I2459	2460–2140 calBCE (3829±30 BP, SUERC-54823)	Amesbury Down, Wiltshire	Great Britain
I2457	2480–2280 calBCE (3890±30 BP, SUERC-36210)	Amesbury Down, Wiltshire	Great Britain
I2457	2200–2031 calBCE (3717±28 BP, SUERC-69975)	Amesbury Down, Wiltshire	Great Britain
I2453	2289–2041 calBCE (3760±35 BP, Poz-83404)	West Deeping	Great Britain
I2445	2137–1930 calBCE (3650±35 BP, Poz-83407)	Yarnton	Great Britain
I2596	2280–2030 calBCE (3739±30 BP, NZA-32484)	Amesbury Down, Wiltshire	Great Britain
I2566	2210–2030 calBCE (3734±25 BP, NZA-32490)	Amesbury Down, Wiltshire	Great Britain
I2452	2195–1920 calBCE (3700±30 BP, Beta-444979)	Dairy Farm, Willington	Great Britain
I2452	2277–2030 calBCE (3735±35 BP, Poz-83405)	Dairy Farm, Willington	Great Britain
I2598	2140–1940 calBCE (3664±30 BP, NZA-32494)	Amesbury Down, Wiltshire	Great Britain
I2460	2030–1820 calBCE (3575±27 BP, SUERC-53041)	Amesbury Down, Wiltshire	Great Britain
I2609	2023–1772 calBCE (3560±40 BP, Poz-83423)	Hexham Golf Course, Northumberland	Great Britain
I2610	1936–1746 calBCE (3515±35 BP, Poz-83498)	Summerhill, Blaydon, Tyne and Wear	Great Britain
I1775	1693–1600 calBCE (3344±27 BP, OxA-14308)	Great Orme Mines, Llandudno, North Wales	Great Britain
I2574	1415–1228 calBCE (3065±36 BP, SUERC-62072)	North Face Cave, Llandudno, North Wales	Great Britain
I2786	2459–2206 calBCE (3850±35 BP, Poz-83639)	Szigetszentmiklós, Felső Űrge-hegyi dűlő	Hungary
I2787	2458–2202 calBCE (3840±35 BP, Poz-83640)	Szigetszentmiklós, Felső Űrge-hegyi dűlő	Hungary
I2741	2458–2154 calBCE (3835±35 BP, Poz-83641)	Szigetszentmiklós, Felső Űrge-hegyi dűlő	Hungary
I4229	2289–2135 calBCE (3775±25 BP, PSU-1750)	Cova da Moura	Portugal
I0826	2833–2480 calBCE (4051±28 BP, MAMS-25940)	Paris Street, Cerdanyola, Barcelona	Spain
I0257	2571–2350 calBCE (3965±29 BP, MAMS-25937)	Paris Street, Cerdanyola, Barcelona	Spain
I0462	2566–2346 calBCE (3950±26 BP, MAMS-25936)	Arroyal I, Burgos	Spain
I0825	2474–2300 calBCE (3915±29 BP, MAMS-25939)	Paris Street, Cerdanyola, Barcelona	Spain

Extended Data Table 2. Sites with new genome-wide data reported in this study.

Site	N	Approx. date range (BCE)	Country
Eton Rowing Course	1	3700–3300	Great Britain
Banbury Lane	3	3360–3100	Great Britain
Totty Pot, Cheddar, Somerset	1	2900–2400	Great Britain
Abingdon Spring Road cemetery, Oxfordshire	1	2500–2200	Great Britain
Hasting Hill, Sunderland, Tyne and Wear	2	2500–1700	Great Britain
Amesbury Down, Wiltshire	10	2500–1400	Great Britain
Windmill Fields, Ingleby Barwick, County Durham	2	2400–1900	Great Britain
Yarnton	4	2400–1900	Great Britain
Staxton Beacon, Staxton, North Yorkshire	1	2400–1600	Great Britain
West Deeping	1	2300–2000	Great Britain
Dairy Farm, Willington, Bedfordshire	1	2300–1900	Great Britain
Over Narrows, Needingworth Quarry, Cambridgeshire	2	2300–1900	Great Britain
Porton Down, Wiltshire	1	2200–1900	Great Britain
Reaverhill, Barrasford, Northumberland	1	2200–1900	Great Britain
Trumpington Meadows	2	2200–1900	Great Britain
Hexham Golf Course, Northumberland	1	2100–1700	Great Britain
Summerhill, Blaydon, Tyne and Wear	1	2000–1700	Great Britain
Thanet, Kent	3	2000–1600	Great Britain
Boscombe Airfield, Wiltshire	1	1800–1600	Great Britain
Canada Farm, Sixpenny Handley, Dorset	1	1500–1300	Great Britain
Macarthur Cave	1	4000–3700	Great Britain
Distillery Cave	3	3800–3300	Great Britain
Raschoille Cave, Oban, Argyll and Bute	6	3800–3200	Great Britain
Tulach an t'Sionnach	1	3700–3500	Great Britain
Tulloch of Assery A	1	3700–3300	Great Britain
Point of Cott, Orkney	2	3700–3100	Great Britain
Clachaig	1	3600–3300	Great Britain
Holm of Papa Westray North	4	3600–3000	Great Britain
Isbister, Orkney	10	3400–2300	Great Britain
Quoyness	1	3100–2900	Great Britain
Dryburn Bridge	2	2300–1800	Great Britain
Eweford Cottages	1	2200–1900	Great Britain
Stenchme, Lop Ness, Orkney	1	2000–1400	Great Britain
Longniddry, Evergreen	3	1500–1300	Great Britain
Pabbay Mor	1	1500–1200	Great Britain
Great Orme Mines, Llandudno	1	1700–1600	Great Britain
North Face Cave, Llandudno	1	1500–1200	Great Britain
Kněževes	2	2500–1900	Czech Republic
Augsburg, Bavaria	2	2800–1800	Germany
Osterhofen-Altenmarkt, Bavaria	1	2600–2000	Germany
Unterer Talweg 58-62, Augsburg, Bavaria	2	2500–2200	Germany
Manching-Oberstimm, Bavaria	1	2500–2000	Germany
Irlbach, County of Straubing-Bogen, Bavaria	2	2500–2000	Germany
Bruck, City of Künzing, Bavaria	2	2500–2000	Germany
Hugo-Eckener-Straße, Augsburg	3	2500–2000	Germany
Unterer Talweg 85, Augsburg, Bavaria	1	2400–2100	Germany
Alburg, Lerchenhaid-Spedition Häring, Bavaria	11	2300–2150	Germany
Budakalász, Csajerszke (M0 Site 12)	2	2500–2200	Hungary
Szigetszentmiklós, Felső Űrge-hegyi dűlő	4	2500–2100	Hungary
Budapest-Békásmegyér	2	2500–2000	Hungary
Samborzec	3	2600–2100	Poland
De Tuithoorn, Oostwoud, Noord-Holland	9	2300–1600	The Netherlands
Via Guidorossi, Parma	1	2200–1900	Italy
Clos de Roque, Saint Maximin-la-Sainte-Baume	3	4700–4400	France
Collet Redon, La Couronne-Martigues	1	3500–3100	France
Hégenheim Necropole, Haut-Rhin	1	2900–2400	France
Dolmen of Villard, Lauzet-Ubaye	2	2459–2242	France
Sierentz, Les Villas d'Aurele, Haut-Rhin	2	2600–2200	France
La Fare, Forcalquier	1	2500–2200	France
Marlens, Sur les Barmes, Haute-Savoie	1	2500–2100	France
Mondelange, PAC de la Sente, Moselle	2	2500–1900	France
Rouffach, Haut-Rhin	1	2400–2100	France
Galeria da Cisterna, Almonda	2	2500–2200	Portugal
Cova da Moura	1	2300–2100	Portugal
Paris Street, Cerdanyola, Barcelona	10	2900–2200	Spain
Camino del Molino, Caravaca, Murcia	4	2900–2100	Spain
Camino de las Yeseras, San Fernando de Henares	2	2280–1790	Spain
Arroyal I, Burgos	5	2600–2200	Spain